

## CFD BASED NUMERICAL MODELING OF DIFFERENT FURNACE CONFIGURATIONS USING AIR STAGING AND REBURNING.

**Ronne Toledo**

Instituto Superior Tecnico, Dep. Eng. Mecânica  
Av. Rovisco Pais, 1049-001 Lisboa, Portugal  
[toledo@navier.ist.utl.pt](mailto:toledo@navier.ist.utl.pt)

**João Luis Toste Azevedo**

Instituto Superior Tecnico, Dep. Eng. Mecânica  
Av. Rovisco Pais, 1049-001 Lisboa, Portugal  
[toste@navier.ist.utl.pt](mailto:toste@navier.ist.utl.pt)

**Abstract.** *The building of new pulverised coal fired plants is expected to occur in fast developing countries in Asia as China, requiring the implementation of efficient and cheap solutions to enhance boiler efficiency with limited NO<sub>x</sub> emissions. This paper presents the contribution of Instituto Superior Tecnico (IST) in the development of alternative supercritical boiler designs. The paper presents results from a Computational Fluid Dynamic (CFD) based numerical model applied to different furnace design using the reburning technology (fuel and air staging). One furnace is conceived with a horizontal configuration with front wall firing with the staged fuel and air in the lateral wall. This new design is compared with a vertical one with opposed wall firing where the gas flow is mainly vertical. For the vertical design the use of the reburning system was compared with the existing air staging principle using overfire air ports. The paper presents for the horizontal furnace the effect of using different firing configurations with burners out of service. For the vertical furnace an optimisation study on the distribution of the overfire air is reported and the global furnace performance of all furnaces design is compared.*

*Keywords.* Modelling, Furnaces, Pulverised coal, Carbon in ash, NO<sub>x</sub> emission.

### 1. Introduction

The implementation of new pulverised coal fired plants is nowadays restricted in Europe and the US due to stringent emissions limits including CO<sub>2</sub>. Fast developing countries in Asia as China however will increase their generating capacity considerably and should use supercritical steam boilers with advanced in-furnace staging technologies to reduce NO<sub>x</sub> emissions at low cost. The use of in-furnace low NO<sub>x</sub> technologies although can not achieve the lower emission levels required by EU and US legislations (200 mg/Nm<sup>3</sup>) for new plants is a cheap technology compared with the use of flue gas treatment. At present the availability of cheaper computational resources and the development of CFD based numerical models, allows their use to analyse burners and furnace design. The CFD models applied to pulverised coal combustion, although can't yet be used as truly predictive tools partly due to the complexity of coal evolution, are valuable tools to compare alternative proposals for furnace designs.

At present comprehensive models as the one used in this paper address the turbulent two phase flow, coupled with the calculation of particle combustion, radiation heat transfer and in a post processor, the formation of NO<sub>x</sub> emissions. At Instituto Superior Tecnico, CFD based numerical models applied to boiler furnaces (Carvalho et al, 1994) were extended to consider pulverised coal combustion (Coimbra et al, 1994) following the examination of the coal sub-models for a burner simulation (Azevedo, 1994). The model was used to examine the influence of the operating conditions of a front wall fired boiler in the NO<sub>x</sub> emissions for different boiler furnaces (Coimbra et al, 1994 and Xu et al, 2000). Using plant data acquired in a Portuguese power plant the model was validated (Coelho, 2003) and the NO<sub>x</sub> post processor calculation procedure was improved to handle not only the case of air staging as well as reburning (Coelho et al, 1997). This model was extensively used in the design of a reburning furnace retrofit performed at Vado-Ligure in Italy (Coelho et al, 1999), which was the first boiler furnace to use this technology where the fuel staged is the same as for the main burners (coal over coal reburning).

The design of the reburning system is a new issue and the use of CFD based models is important to analyse gas mixing in the furnace to guarantee a good staging efficiency. Therefore the project was based on the experience from the Vado-Ligure demonstration project and on the use of CFD simulations to compare alternative configurations. The CFD based model can provide data on gas mixing and calculate global performance characteristics such as carbon in ash and NO<sub>x</sub> emissions for different furnace configurations. In the present paper a comparison is performed between three different furnace configurations. The use of reburning technology is considered for a horizontal furnace design and for a more conventional vertical design. For the vertical design the use of reburning is compared with the use of air staging, considered as the base case. The CFD model is used to optimise the air distribution and to analyse the use of burners out of service.

In the following section the paper presents briefly the mathematical model used and the calculation of the specific parameters used in the analysis. Section 3 presents the configurations considered and the two following sections present detailed model results. Section 4 includes a discussion on the optimisation of overfire air distribution. Section 5 examines the location of the reburning system and the use of burners out of service for the horizontal design. Section 6 presents a summary of the global results of the numerical simulations and the final section presents conclusions on the relative merits of the different solutions.

## 2. Mathematical Modeling

The numerical model is based on the Favre averaged 3-D transport equations applied to the momentum components, closed with the k- $\varepsilon$  turbulence model. The continuity equation is used to calculate pressure according to the Simple algorithm. The equations mentioned are used to calculate the turbulent flow taking into account the mass sources from the particulate phase. The general form of the transport equation (Versteeg and Malalasekera, 1995) is presented in Eq. (1) and is used to calculate the variables presented in Tab. (1) including the three momentum components, turbulence energy and its dissipation rate, enthalpy, the mass fraction of gaseous fuel and its variation. The coefficients of the turbulence model including combustion are presented in Tab (2) and follow the proposal of Lockwood and Naguib (1975), while the Schmidt numbers used are presented in Tab. (3).

$$\frac{\partial(\rho u_i \phi)}{\partial x_i} = \frac{\partial}{\partial x_i} \left( \Gamma_\phi \frac{\partial \phi}{\partial x_i} \right) + S_\phi \quad (1)$$

Table 1. Variable and source term for transport equation

$\phi$	$\Gamma_\phi$	Variable	$S_\phi$
$u_i$	$\mu_e$	Momentum component	$-\frac{dP}{dx_i} + (\rho_0 - \rho)g_i + \frac{\partial u}{\partial x_j} \left[ \mu_e \frac{\partial u_j}{\partial x_i} \right]$
$k$	$\frac{\mu_t}{\sigma_\kappa}$	Turbulent kinetic energy	$G_k - \rho\varepsilon$
$\varepsilon$	$\frac{\mu_t}{\sigma_\varepsilon}$	Dissipation rate of turbulent kinetic energy	$(C_{1\varepsilon}G_k - C_{2\varepsilon}\rho\varepsilon) \frac{\varepsilon}{k}$
$h$	$\frac{\mu_t}{\sigma_h}$	Enthalpy	$S_{\text{Rad}} + S_{\text{Part}}$
$f$	$\frac{\mu_t}{\sigma_f}$	Mixture fraction	$S_{\text{Vol}} + S_{\text{Char}}$
$g$	$\frac{\mu_t}{\sigma_g}$	Variation of mixture fraction	$C_{g1}\mu_t \left[ \left( \frac{\partial f}{\partial x} \right)^2 + \left( \frac{\partial f}{\partial y} \right)^2 + \left( \frac{\partial f}{\partial z} \right)^2 \right] - C_{g2}\rho g \frac{\varepsilon}{\kappa}$

Table 2. Coefficients used on the source terms from Tab. (1).

$G_k$	$\mu_t$	$\mu_e$	$C_\mu$	$C_{1\varepsilon}$	$C_{2\varepsilon}$	$C_{g1}$	$C_{g2}$
$\frac{1}{2} \mu_t \left[ \frac{\partial u_i}{\partial x_j} + \frac{\partial u_j}{\partial x_i} \right] \left[ \frac{\partial u_i}{\partial x_j} + \frac{\partial u_j}{\partial x_i} \right]$	$\rho C_\mu \frac{\kappa^2}{\varepsilon}$	$\mu + \mu_t$	0,09	1,44	1,92	2,80	2,00

Table 3. Diffusion coefficients for the balances indicated in Tab. (1).

$\sigma$	$\sigma_\varepsilon$	$\sigma_\kappa$	$\sigma_f$	$\sigma_g$	$\sigma_h$
	1,30	1,00	0,7	0,7	0,7

The gas properties are calculated from the mixture fraction (f) and its variation (g) assuming a clipped Gaussian distribution. The mass sources from the particulate phase are considered in the continuity equation and in the mixture fraction equation. The use of the mixture fraction for the gas phase combustion does not distinguish the volatiles ( $S_{\text{Vol}}$ ) from the carbon monoxide produced from char combustion ( $S_{\text{Char}}$ ) but is a computational robust approach. For the energy balance, source terms are considered from the heat exchanged with the particles ( $S_{\text{Part}}$ ) and by radiation ( $S_{\text{Rad}}$ ). The radiation heat transfer is held using the discrete heat transfer algorithm.

The particulate phase is described using a Lagrangian formulation, where the trajectories of representative coal particles are calculated from the momentum balance presented in Eq. (2). This integration is performed using instantaneous gas velocities, stochastically selected with a Gaussian distribution around the mean value. The velocity fluctuation and the characteristic time scales of these are calculated using the turbulence model.

$$\frac{\partial(m_p \vec{u}_p)}{\partial t} = A_{pt} \frac{\rho}{2} C_D |\vec{u} - \vec{u}_p| (\vec{u} - \vec{u}_p) + m \vec{g} \quad (2)$$

Along the particle trajectories an energy balance to the particle is also solved to calculate its temperature and to describe the different stages of coal evolution. Equation (3) presents the energy balance equation with heat transfer by convection and radiation and an energy source due to particle drying and heterogeneous combustion.

$$\frac{d}{dt}(m_p c_p T_p) = A_p [h(T - T_p) + \sigma \varepsilon_p (T^4 - T_p^4)] + \frac{dm_{H_2O}}{dt} H_{H_2O} + \frac{dm_{ch}}{dt} H_{ch} \quad (3)$$

The model considers in sequence coal drying, devolatilisation and char combustion. Devolatilisation was described by the two parallel reactions mechanism of Ubhayakar et al (1977), while char combustion was described by a first order apparent reaction with the following coefficients:  $A_c=0,288\text{kg/m}^2\text{sPa}$  and  $E_c=8,372\text{E}+4 \text{ kJ/kmol}$ , proposed by Smith (1982). The trajectories are calculated until the coal particles are completely converted or in case they are not completely burnt if they are trapped close to the furnace walls or exit through the furnace exit. The total amount of carbon in the particles not completely converted represents a combustion loss. The unburned carbon is mixed with the ash collected from the furnace and its concentration is named unburned carbon in ash (CIA) that is an important parameter to control. To use the ash for cement applications requires that the level of CIA should be lower than 5%. The calculation of carbon in ash is directly influenced by the assumption made for the particle behaviour when they impact the wall and by the char burnout model parameters.

The  $\text{NO}_x$  calculations were performed using a pos-processing routine based on De'Soete (1975) mechanism for the volatile components containing nitrogen. This mechanism applied to the  $\text{NO}_x$  precursors ( $\text{HCN}$  and  $\text{NH}_3$ ) can be identified in Fig. (1) with competitive reactions with  $\text{O}_2$  or with  $\text{NO}$  leading to the formation of  $\text{NO}$  or  $\text{N}_2$ . Following devolatilisation part of the nitrogen remains in the solid residue that will be oxidised more slowly. Half of the nitrogen from the char was assumed to release as  $\text{NO}_x$  precursors participating in the De'Soete mechanism while the other half was considered to oxidise at the char surface. A mass balance was established considering this oxidation and the reduction in the char surface to yield the final production of  $\text{NO}$  from the char. Further to the fuel mechanism described, the  $\text{NO}_x$  model was extended to consider the thermal  $\text{NO}_x$  mechanism (reaction 7) and the reburning mechanism (reaction 5). Methane ( $\text{CH}_4$ ) is one of the volatile components estimated as 10% of the total volatiles that reduces the  $\text{NO}$  already present in the gases to  $\text{HCN}$  that is again subject to the De'Soete mechanism. The production of these reactions in a region with low oxygen concentration reduces  $\text{NO}$  concentration by the reburning mechanism.

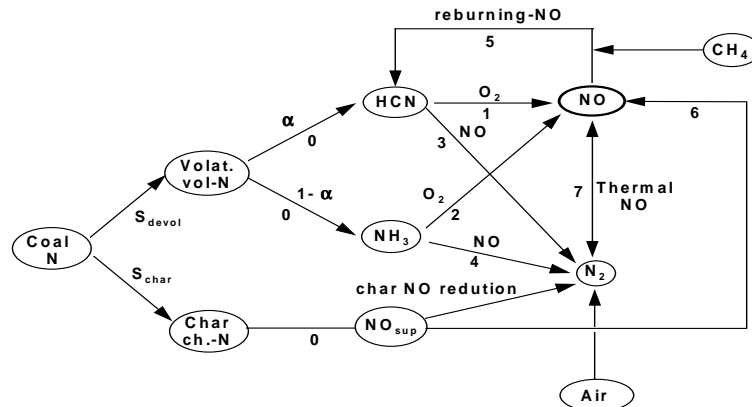


Figure 1. Schematic representation of the  $\text{NO}_x$  formation model.

### 3. Furnace Designs and Operations Conditions

Figure (2) shows the vertical and horizontal (half geometry with symmetry plane) cases tested on this work. The grids considered in the simulations were respectively:  $44 \times 75 \times 95$  for case MB RB OFA,  $40 \times 71 \times 110$  for MB OFA and  $101 \times 27 \times 75$  for the half furnace of the horizontal furnace. The Fig. also shows the representation of the inlet ports.

The vertical furnace designs, considered here, are opposed wall fired. Five rows of main burners were considered (2 in the front wall and 3 in the back wall) according to Fig. (2). The main combustion zone is defined up to the level of the reburning burners that are located in the same front and back walls, but are smaller due to their lower capacity. The reburning zone is defined between the reburning burners level and the level of the over fire air (OFA) ports that in this design are located on the lateral walls. Two different configurations were considered for the over fire air injection with 6 or 7 OFA ports. The OFA zone is considered as the space between the OFA ports and the inlet plane to the superheater panels. The nomenclature used here to identify this case is MB RB OFA (**M**ain **B**urners **R**e**B**urning and **O**ver **F**ire **A**ir ports). Simulations were performed for a similar case but without considering the use of the reburning ports, corresponding to a case with air staging referred as MB OFA B. The furnace designed for the use of air staging considers the position of the over fire air ports, closer to the main burners and located above the main burners in the front and back wall. This case is identified as MB OFA A (**M**ain **B**urners and **O**ver **F**ire **A**ir ports).

The other furnace design considered was designed for the same operating conditions as the vertical furnace but with the main flow in the horizontal direction. The main burners are positioned in the front wall, while the reburning burners and OFA ports are located on the lateral walls. The column of the reburning ports was considered at two distances from the front wall, the nearest one designated here by A and the other by B. In both cases the distance from these burners to the OFA ports was fixed. For the horizontal case due to the symmetry only half furnace was considered with a symmetry plane on the middle of the furnace.

For all cases, the operation conditions considered correspond to 600MW electrical capacity. The reburning burners feed 20% of the total coal flow rate, using air and recirculated flue gases to produce a better distribution in the furnace. These burners have a lower capacity and operate with sub-stoichiometric conditions. In the reburning case the staged air corresponds to 25% of the total, this value being reduced to 16% when reburning is out of service. For the air staging design the over fire air flow is 12% of the total. For the reburning case in the vertical furnace two different distributions of over fire air ports were considered, respectively with 6 and 7 ports in the lateral wall. For each case, the flow distribution in the staged air ports was varied to optimize the efficiency of the reburning system as will be presented in section 4.

For the horizontal furnace the flow distribution is similar to the vertical reburning case. Two different strategies were considered for the use of burners out of service, depending on the arrangement of the coal mills. In all cases with burners out of service the coal and air flow was equally divided by the similar ports in operation, keeping some air flow in the ports out of service for cooling purposes. Considering four coal mills, each one feeds a row of main burners and reburning ports, so when the main burner row is out of service so it is the correspondent reburning port. This case is identified as A1 and B1 and considers also the correspondent ports of over fire air out of service. Another alternative is to consider independent coal mills for the reburning system and in this case when a row of main burners is out of service all the reburning and OFA ports are considered in service, corresponding to the cases CRC presented.

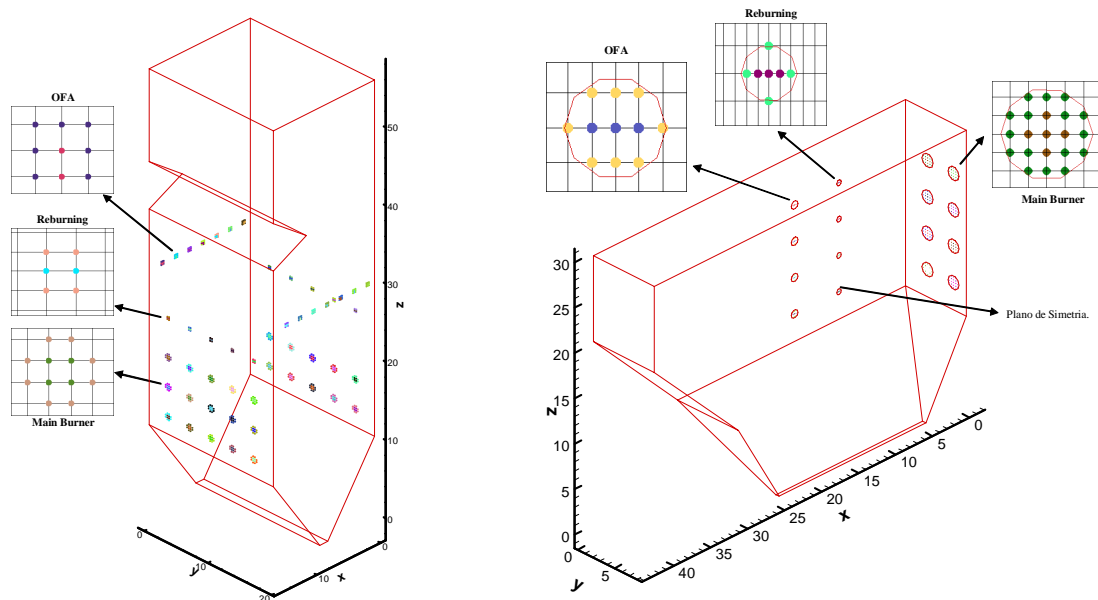


Figure 2 – Schematic representation of the vertical and horizontal furnace, showing the location of the inlet ports.

#### 4. Vertical Furnace Design

Figure (3) presents the oxygen distribution in a central vertical plane across the center of the furnace for the case of air staging and two cases with reburning using 7 ports at each side of the furnace. For the case with air staging recirculated flue gases for sealing were considered at the ash hopper, that was neglected in the cases with reburning. For the air staging case the flames are longer due to the higher air flow rate and higher temperature achieved in the main burner flames. The thermal input in all the burners is similar as only four rows of burners were considered in operation for the reburning cases, while for air staging all the five rows were considered in operation. The upper burner row for the reburning cases has some cooling air that leads to local higher values of oxygen concentration, shown in Fig. (3) (b) and (c). The main burners flow is deflected by the opposite flow leading to recirculations at the ash hopper.

The staged air in the front and back wall in the air staged case have a good penetration in the furnace but is consumed more rapidly in the front wall due to the larger number of burners in the back wall. No optimization was done for this case but the use of higher air flow in the front wall or the use of more burners in the front wall should improve mixing. The use of the reburning ports in the front and back wall do not provide a full penetration in the furnace as well as the overfire air flow for the case shown in Fig. (3) (b). For this case the overfire air flow reaches the center of the furnace only for the ports close to the front and back wall. Therefore an optimization of the air flow distribution was performed.

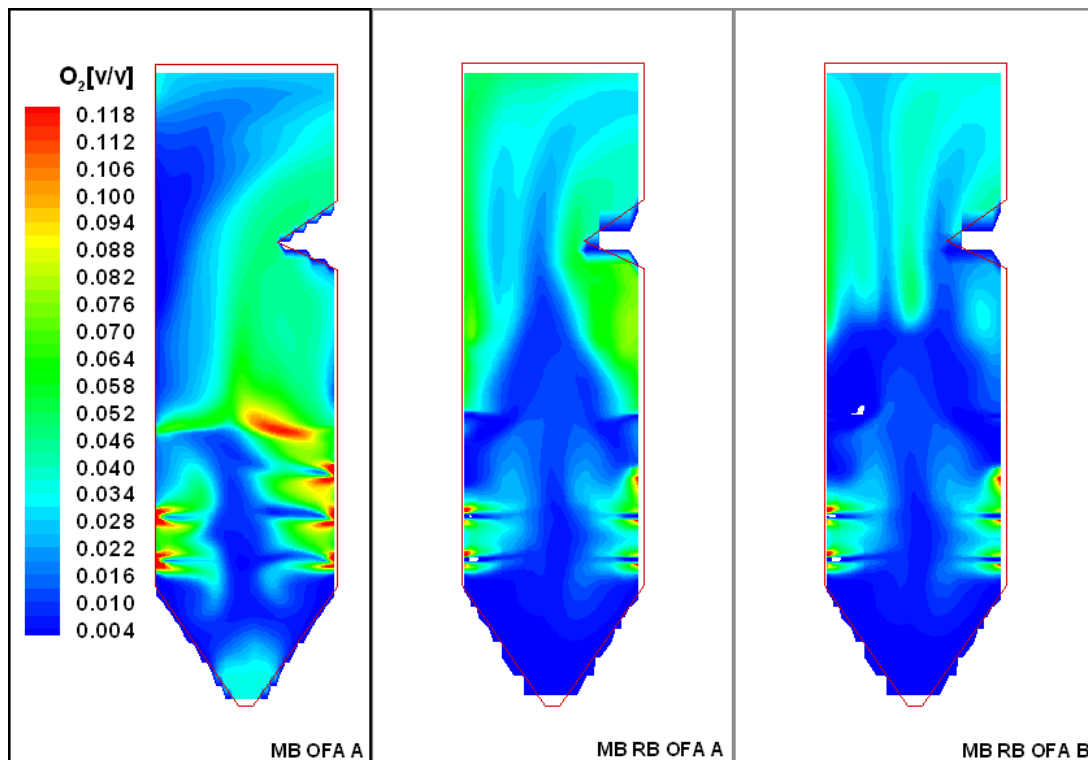


Figure 3- Oxygen distribution in the central vertical plane of the furnace. a) Air staging, b) Reburning with uniform over fire air flow distribution, c) Reburning with optimized over fire air flow distribution.

The efficiency of the air staging system depends on the penetration and mixing of the air jets injected through these ports. This is important to confine the reburning zone with a low stoichiometry and therefore back mixing from the over fire air system should be avoided. In the present study an optimization of the over fire air system was performed keeping the main and reburning burners operating conditions. Figure (4) shows the velocity distribution in the horizontal plane crossing the over fire air ports for different cases considered. The color isolines correspond to the vertical velocity component that has negative values close to the front and back wall and are larger at the center of the furnace. The results in Fig. (4) (a) and Fig. (4) (b) respectively correspond to the case with 6 ports (MB RB OFA D) and with 7 ports (MB RB OFA A), considering in both cases the total air flow equally divided for all ports. The air velocity is higher when using a smaller number of ports and there is a strong interaction between the jets close to the front and back wall. In both cases the OFA jets do not reach middle of furnace due to the deflection of the upward flow as can be seen in Fig. (3) (b).

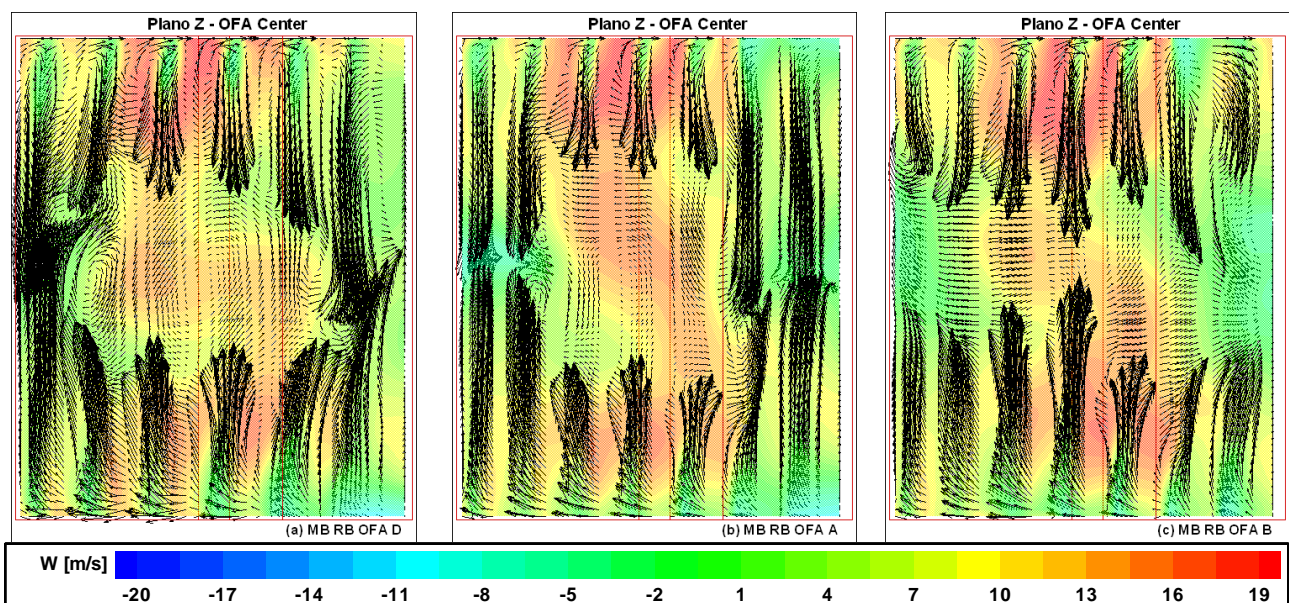


Figure 4 - The cross plane on Z axis on the OFA ports position. (a) the case MB RB OFA D, (b) the case MB RB OFA A and (c) MB RB OFA B.



To increase the penetration of the OFA jets on the middle of the furnace another case was calculated with a redistribution of air flow using as reference the size of the vector arrow shown in Fig. (4) (b). The total amount of air flow injected in the OFA was the same, but the air flow in the lateral ports was transferred to the central ports using as a factor the difference between the size of each vector and the average vector for all ports shown in Fig. (4) (b). Using proportionality factor the flow in each port was divided as 10,5%, 11,0%, 18,0%, 21,0%, 18,0%, 11,0%, 10,5% for each port. This case is named MB RB OFA B, and the result is shown in Fig (4) (c). The consequence of a better flow distribution in the OFA ports leads to a more effective oxygen concentration distribution as seen from Fig. (3) (c).

The examination of the flow distribution is useful but does not provide a quantitative comparison among the different cases. The mixing of the OFA flow was quantified by calculating a mixture factor between the air injected by the OFA ports and the total gas on the furnace. The sum of the absolute differences between the calculated mixture fraction and the average value at the furnace exit, divided by the average value, provides a mixing factor between 0 and 1 corresponding respectively to the case of perfect mixing and no mixing.

The average value of the mixing factor along the furnace height is represented in Fig. 5, for the cases presented above in Fig. (4). This figure shows that after the OFA injection plane, mixing is improved for case B, compared with the cases with uniform flow. As mentioned before the case with 6 lateral ports (D) has poorer mixing than with 7 ports (A). Below the level of the OFA ports injection there is some back mixing as can be seen by the values lower than 1. The back mixing is higher for the case with 7 ports due to the negative velocity components in the vertical direction that drag over fire air from the jets close to the front and back wall.

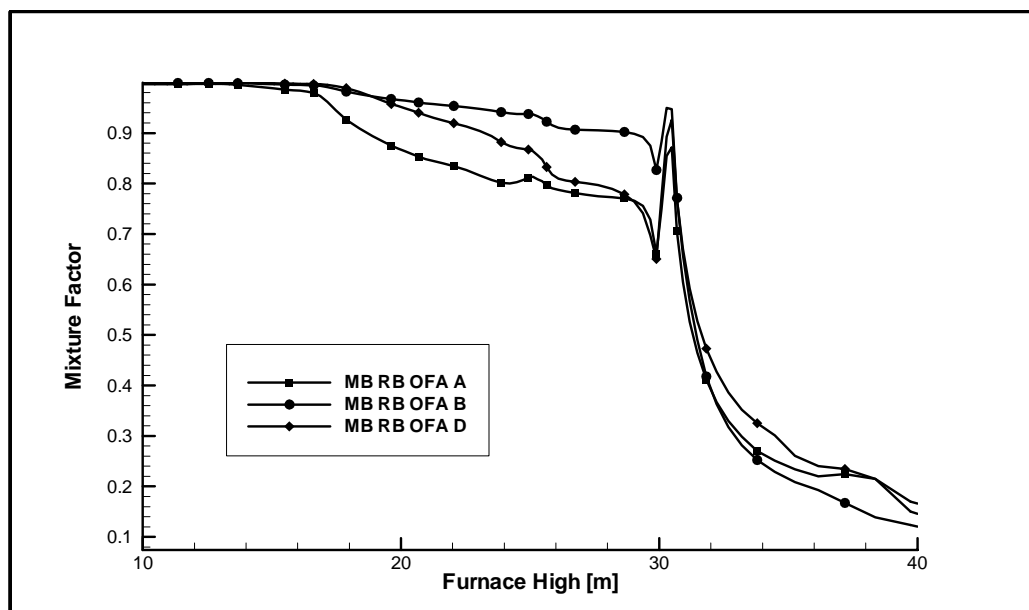


Figure 5 - Average mixture factor along the furnace height for the cases MB RB OFA presented in Fig. (4).

Figure (6) presents the NO concentration profiles at the center of the furnace for the cases presented in Fig. (3). From this figure it can be observed that NO formation at the main combustion zone is higher for the cases with reburning. This is due to the higher combustion intensity as can be observed by the lower oxygen concentration in Fig. (3). The air/fuel ratio for both cases is similar in the main combustion zone but the flow from the reburning case is smaller in the main combustion zone. The introduction of the over fire air in the air staging case dilutes the nitric oxide from the main combustion zone but the final value are clearly higher than the reburning cases. The reburning burners produce an effective reduction of NO, specially in case B5, due to a good mixture of the staged coal in the main flow. From Fig. (3) and (6) it can be observed that the mixing from the reburning ports could also be improved. The penetration of the over fire air ports for case B5 is much more effective than in case A5 as anticipated. The poorer reduction efficiency of the reburning coal in case A5 is partly a consequence of the mixing of over fire air in the reburning zone, increasing the effective stoichiometry in that zone.

Further to gas mixing and NOx formation, the CFD model allows for the analysis of the contribution of burners for the values of carbon in ash (CIA). Table (4) presents for the case of air staging and the optimized case with reburning the of unburned carbon from each individual burner. It can be easily identified that the main contribution for the unburned carbon is from the lower wing burners. In fact particle trajectories from the lower burners are deflected into the ash hopper and have higher impact rates onto the boiler walls. Table (4) also shows that the coal particles from the reburning ports have comparable burnout as for the other ports. This is a consequence of the good mixing from the over fire air. Figure (7) shows the mass fractions of the coal from the reburning ports consumed in each furnace zone. From this Fig. (7) it can be observed that a significant fraction of the coal is burned in the main combustion zone due to flow recirculation close to the reburning ports. The coal from the main burners is also not completely consumed in the main combustion zone, so the use of the CFD model is important to analyze the coal combustion in the furnace.

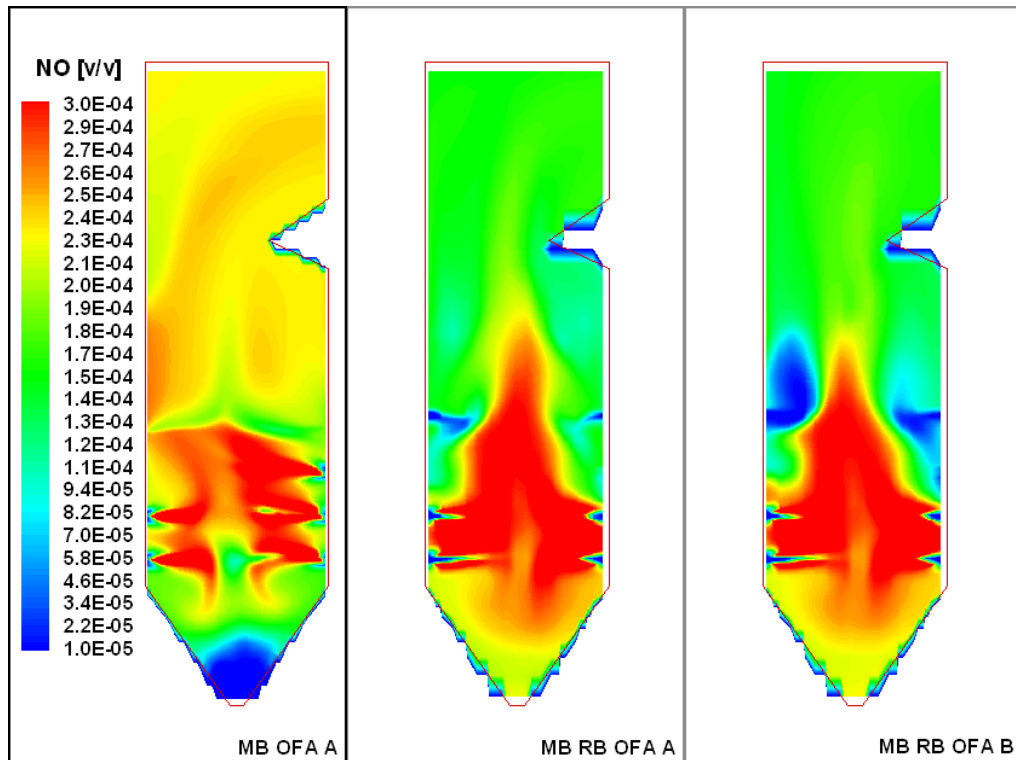


Figure 6 – NO concentration distribution in the central vertical plane of the furnace. a) Air staging, b) Reburning with uniform over fire air flow distribution, c) Reburning with optimized over fire air flow distribution.

Table 4 – Mass fraction of unburned carbon from individual burners for a) Air staging, b) Optimized reburning.

Case	Front Wall					Back Wall				
Staged coal	26	27	28	29	30	31	32	33	34	35
MB RB OFA B	0.06%	0.22%	0.37%	0.11%	0.66%	0.15%	0.19%	0.08%	0.01%	0.03%
3 <sup>rd</sup> burner row						21	22	23	24	25
MB OFA A						1.12%	0.03%	0.35%	0.02%	0.22%
MB RB OFA B										
2 <sup>nd</sup> burner row	11	12	13	14	15	16	17	18	19	20
MB OFA A	2.95%	0.15%	0.05%	0.29%	2.42%	3.28%	0.64%	0.13%	0.05%	2.12%
MB RB OFA B	0.44%	0.04%	0.01%	0.05%	0.87%	0.78%	0.08%	0.02%	0.05%	0.39%
3 <sup>rd</sup> burner row	1	2	3	4	5	6	7	8	9	10
MB OFA A	4.57%	0.29%	0.25%	0.75%	2.28%	1.45%	0.45%	0.16%	0.26%	5.30%
MB RB OFA B	3.57%	0.49%	0.50%	0.84%	2.13%	1.79%	0.90%	0.50%	0.51%	2.21%

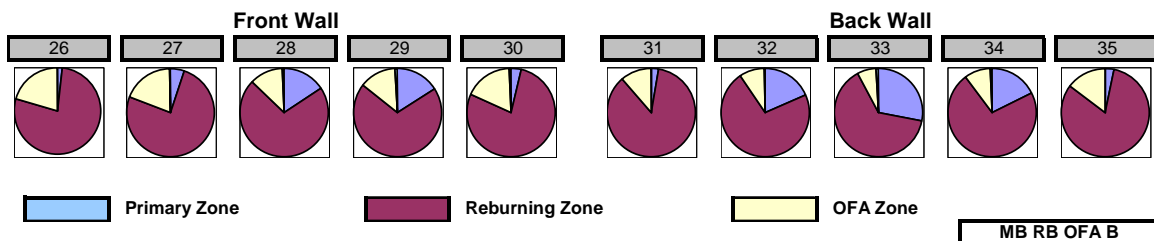


Figure 7 – Mass fractions of the coal from the reburning ports consumed in each furnace zone and unburned.

## 5. Horizontal Furnace Design

The horizontal furnace design has the objective of achieving a lower construction cost but is not an usual furnace configuration for multi-burners applications. As mentioned in the presentation of the cases, two distances were

considered for the location of the reburning system and for each one the use of burners out of service was considered. Figure (8) shows the oxygen concentration distribution in representative planes for the reburning system for both distances from the main burners with all burners in operation. The location of the reburning ports closer to the front wall, lead to an important mixing between the main and reburning burners, so there is no effective fuel staging as can be seen by the oxygen distribution in the horizontal plane presented. Considering the reburning system located further downstream, lower oxygen concentration are achieved before the reburning injection, indicating a more complete combustion from the main burners. The reburning flow in this case forms a curtain limiting the main burner region while in case A the reburning flow merges with the main burners flow and close to the furnace wall and center mixing is limited. Figure (8) shows that in both cases the penetration of the over fire air flow is strong reaching the center of the furnace without significant mixing. A better mixing could be obtained increasing the swirl of the outer over fire air ports. The consideration of all the furnace in the simulation would also generate interactions between the impinging over fire jets improving mixing.

Figure (9) shows the NO concentration distribution in the horizontal furnace for the two distances of the reburning system from the front wall. When the reburning system is located closer to the front wall, NO is further formed from the volatiles of the staged coal due to higher oxygen concentration. For case B, the formation of NO is larger in the main combustion zone due to the higher coal conversion from the main burners, seen from the lower oxygen concentration in Fig. (8). The reburning coal releases volatiles that are then responsible for the reduction of NO from the main combustion zone. In fact for case B, NO concentration is further reduced when compared with case A. The analysis of the mass fraction conversion in each combustion zone (not presented) shows that for case B the conversion of the coal from the front wall burners in the main combustion zone is above 95% while for case A is around 85%. Therefore the staging in case A is not so effective limiting the efficiency of NO reduction from the reburning system.

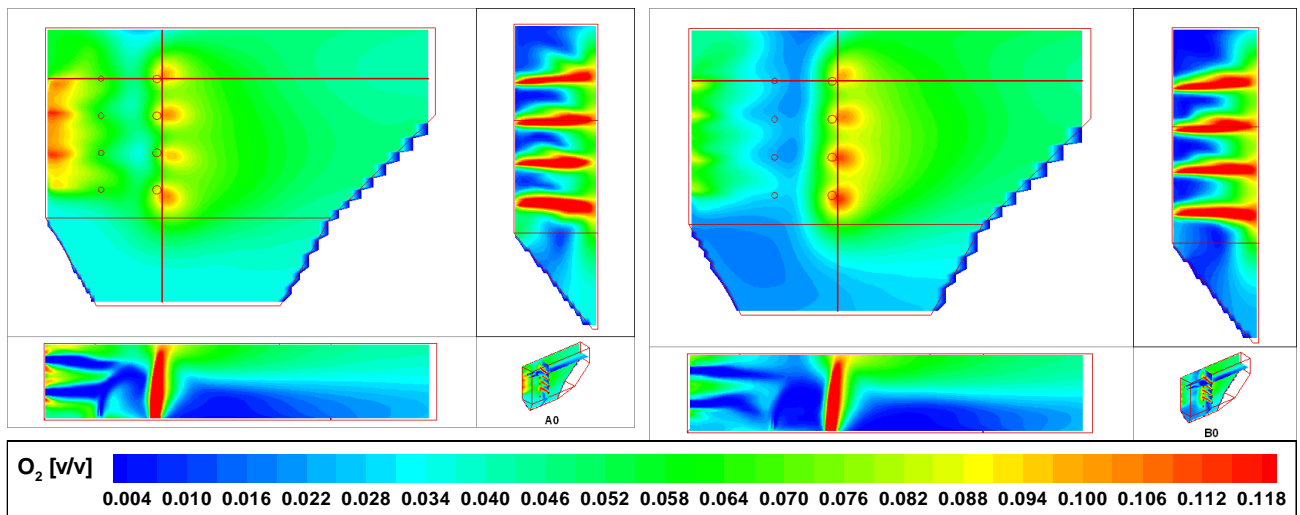


Figure 8 – Oxygen concentration distribution for the horizontal furnace a) Case A, b) Case B.

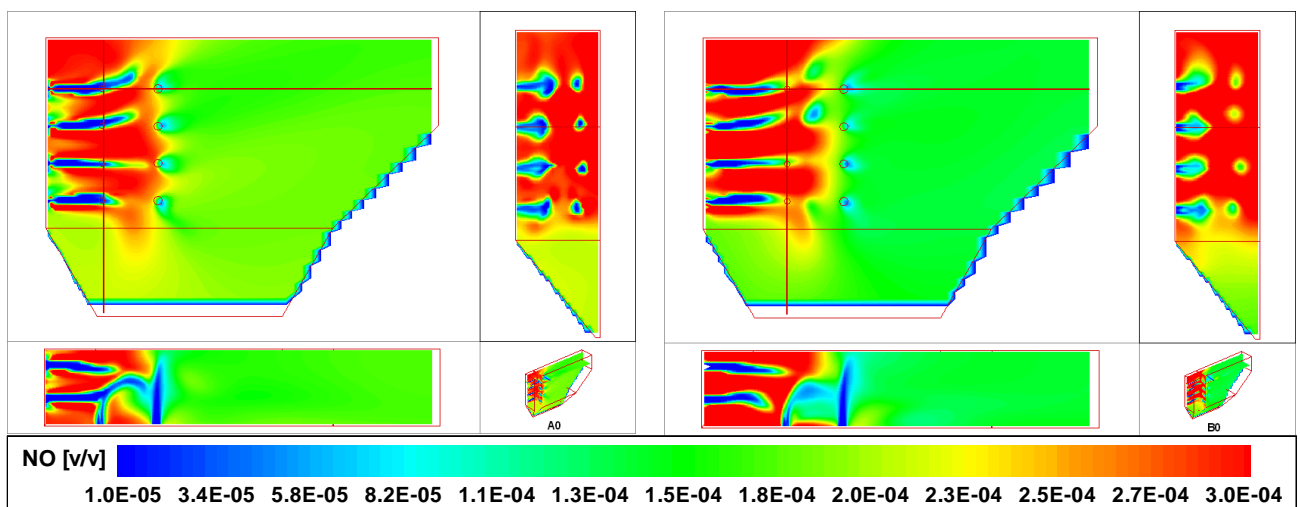


Figure 9 – Nitric oxide concentration distribution for the horizontal furnace a) Case A, b) Case B.

Different strategies were considered for the use of burners out of service in the horizontal furnace as discussed before. Figure (9) presents the oxygen concentration distribution for the case of the reburning system closer to the front



wall. In the left case, the first level of main burners, reburning and OFA ports are considered out of service, while in the right case only the lower level of main burners is out of operation. For the left case (A1) with only three rows of the reburning system in operation, the interaction between the main and staged burners is similar to the case of all burners in operation and there is also a mixing between the burners flow. For the right case (A1-CRC) the flow in the reburning ports is smaller and a stronger recirculation flow in the ash hoper is formed, leading to a large oxygen concentration in the upper region of the furnace with lower temperature (not shown). For this case most combustion occurs close to the over fire air ports where mixing is larger and there is no fuel staging effects.

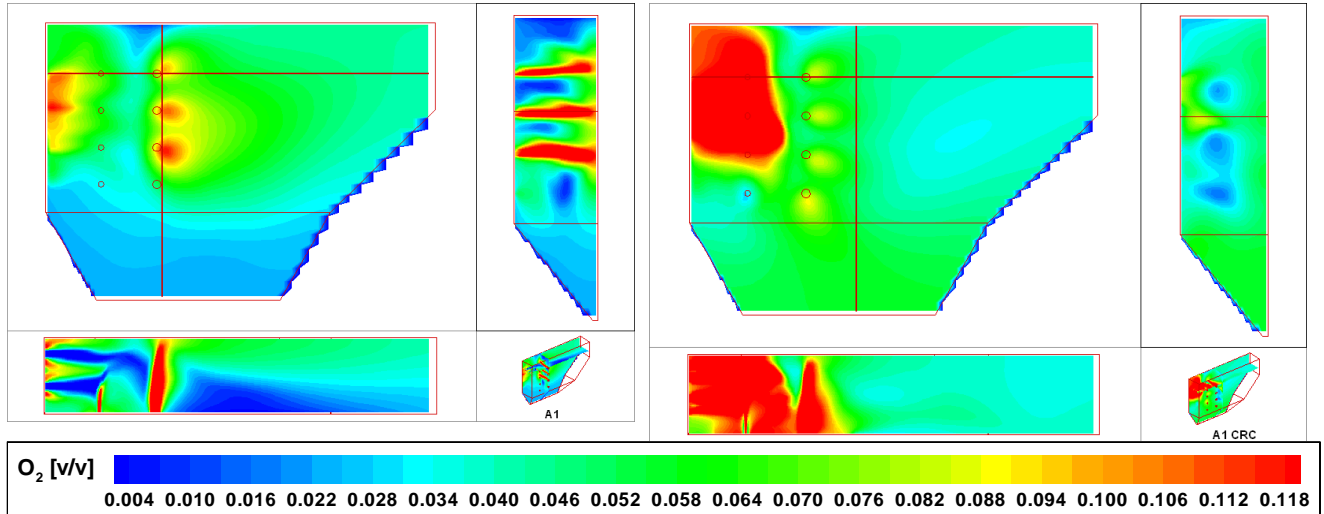


Figure 10 – Oxygen concentration distribution for the horizontal furnace with the lower row of main burners out of operation a) Lower row of the reburning out of service, b) All ports of reburning system in operation.

## 6. Global result and discussion

Table (5) shows a summary of the main results from the cases tested. Further cases are presented by Toledo (2003) including the simulation of partial load operation. The furnace exit gas temperature (FEGT) is rather similar among all cases, while the temperature in the plane corresponding to the panels (FEPT) is larger for the cases with the reburning ports closer to the front wall. This result is due to a merge of the flame from the main burners as it was observed in Fig. (8). The total heat transfer by convection ( $Q_{Conv}$ ) is larger for the vertical furnace due to the larger area and because in the case of the horizontal furnace the flow is pushed towards the center of the furnace. The total absorbed radiation heat flux ( $Q_{Rad}$ ) is similar in all cases with lower values for the cases CRC where combustion is delayed.

Table 5 – Main results from the cases tested.

	FEPT	FEGT	QConv	QRad	CIA	O2	NOx
	(°C)		[MW]		%	(% v/v)	mg/Nm <sup>3</sup> @6% O2
MB OFA A	1191	1027	77	641	11,93	3,39	402
MB OFA B	1134	1021	79	659	10,68	3,33	458
MB RB OFA D5	1125	1021	81	616	8,02	3,28	279
MB RB OFA A5	1122	1022	80	616	6,66	3,36	294
MB RB OFA B5	1114	1005	82	625	6,80	3,37	276
A0	1216	1041	57	647	1,71	3,27	305
A1 CRC	1332	1092	52	572	12,23	3,65	508
A1	1241	1047	65	615	2,67	3,33	365
B0	1165	1014	58	638	3,33	3,35	245
B1 CRC	1260	1068	56	603	7,82	3,49	441
B1	1195	1025	65	626	3,75	3,39	352

The CRC cases also have higher values of carbon in ash (CIA) showing lower coal combustion efficiency. The lower values are obtained for the horizontal furnace due to intense mixing of the main flow stream with the flow from the lateral ports. For the vertical furnace the large values of CIA are a result of the impact rate of particles in the walls, mainly in the lower section of the furnace, that are higher for the cases of air staging.

The NO concentration in the flue gas calculated was the lowest for the horizontal furnace (case B0) but increased considerably with the use of burners out of service due to by-pass effects. The location of the reburning system closer to the front wall also increased NO concentration because the staging effect was lost. The results show clearly that the NO formation with reburning is smaller than using only air staging. The operation with air staging for the reburning configuration (MB OFA B) led to the worst results due to the large area of the main combustion zone and low mixing of the over fire air. For the vertical furnace with reburning as mentioned an optimization of the over fire air flow distribution was performed. From Tab. (5) it can be observed that all the values obtained are low and similar although they are better for case B5.

## 7. Conclusions

A CFD model was applied to three furnace configurations corresponding to similar operating conditions allowing for their comparison in terms of gas mixing, heat transfer (not analyzed here), carbon burnout and NO formation. This is one example of the use of CFD models, whose results however should be analyzed with care.

The NO formation using the reburning technology is about 35% lower than using air staging. Small improvements could be obtained by optimizing the distribution of the over fire air by their ports. In particular the back mixing of the over fire air into the reburning zone was found to be a critical factor. For the vertical furnace configuration, the main contribution for unburned carbon was found to result from the lower wing burners that may have large impact rates in the ash hopper.

The horizontal furnace design was examined and compared with more conventional vertical configurations, showing that the impact of particles on walls is lower. Two distances of the reburning system from the front wall were compared, the closer leading to a mixing of the main and reburning burners while the second led to an effective fuel and air staging. The NO formation in this configuration was lower but was found to be very sensitive to the use of rows of burners out of service.

## 8. References

- Azevedo, J.L.T., 1994, "Modelação Física e Simulação Numérica de Sistemas de Queima de Combustíveis Sólidos", PhD Thesis, Instituto Superior Técnico, Universidade Técnica de Lisboa.
- Carvalho, M.G., Coelho, P.J., Moreira, A.L.N., Silva, A.M.C. and Silva, T.F., 1994, "Comparison of Measurements and Predictions of Wall Heat Flux and Gas Composition in an Oil-Fired Utility Boiler", 25<sup>th</sup> Symposium (Int.) on Combustion, The Combustion Institute, pp. 227-234.
- Coelho, L.M.R., Azevedo, J.L.T. and Carvalho, M.G., 1997, "Application of a Global NO<sub>x</sub> Formation Model to a Pulverised Coal Fired Boiler with Gas Reburning", 4<sup>th</sup> Int. Conf. on Technologies and Combustion for a Clean Environment, Lisboa.
- Coelho, L.M.R., Carvalho, M.G., Pasini, S., Antifora, A., Schnell, U. and Hesselman, G., 1999, "Numerical Modelling Applied to the Design of a Coal-Over-Coal Reburn Process at Vado Ligure Unit #4 (320 MWe)". 4<sup>th</sup> International Symposium on Coal Combustion, Beijing, China.
- Coelho, L.M.R., 2003, "Simulação numérica de métodos de redução de emissões de NO<sub>x</sub> em caldeiras de carvão pulverizado", PhD Thesis, Instituto Superior Técnico, Universidade Técnica de Lisboa.
- Coimbra, C.F.M., Azevedo, J.L.T. and Carvalho, M.G., 1994, "3-D Numerical Model for Predicting NO<sub>x</sub> Emissions From a Pulverised Coal Industrial Boiler", FUEL, 73(7): 1128-1134.
- DeSoete, G. G., 1975, "Overall Reaction Rate of NO and N<sub>2</sub> Formation From Fuel Nitrogen". 15 Symposium (Int.) on Combustion, The Combustion Institute, pp. 1093-1102.
- Lockwood, F.C., and Naguib, A.S., 1975, "The prediction of the fluctuations in the properties of free round jet turbulent diffusion flames", Combustion and Flame, Vol. 24, pp.109-124.
- Versteeg, H.K., and Malalasekera, W., 1995, "An Introduction to Computational Fluid Dynamics - The finite volume method", Ed. Longman Scientific & Technical.
- Smith, I. W., 1982, "The Combustion Rates of Coal Chars: A Review" 19<sup>th</sup> Symposium (Int.) on Combustion, The Combustion Institute, pp1045-1065.
- Toledo, R., 2003, "Modelação e Comparação Numérica de Diferentes Configurações de Fornalhas de Carvão Pulverizado", Master Thesis, Instituto Superior Técnico, Universidade Técnica de Lisboa.
- Ubhayakar, S.K., Stickler, D.B., Rosenberg, C.W. and Gannon, R.E., 1977, "Rapid Devolatilization of Pulverised Coal in Hot Combustion Gases", 16<sup>th</sup> Symposium (Int.) on Combustion, The Combustion Institute, pp 427-436.
- Xu, M., Azevedo, J.L.T., e Carvalho M.G., 2000, "Modeling of the Combustion Process and NO<sub>x</sub> Emission in a Utility Boiler", Fuel, Vol. 79, pp. 1611-1619.

## 9. Acknowledgements

The authors would like to express their gratitude to the financial support of the European Commission contract Energy – NNE5/1999/310: ISB-2000 – Innovative Supercritical Boilers for Near Term Global Markets and to the partners: Babcock Energy, Siemens, ENEL and Power Gen. The opinions expressed in the paper are exclusively from IST.